HETEROCYCLES, Vol. 106, No. 3, 2023, pp. 439 - 454. © 2023 The Japan Institute of Heterocyclic Chemistry
Received, 21st December, 2022, Accepted, 25th January, 2023, Published online, 2nd February, 2023
DOI: 10.3987/COM-22-14801

DESIGN, SYNTHESIS, AND BIOLOGICAL EVALUATION OF NEW DI-ARYLIMIDAZOLE-QUINAZOLINONE HYBRID

Parsa Moghimirad,[a] Shahin Boumi,[a] Seyed Nasser Ostad,[c] Maliheh Barazandeh Tehrani,[a]* and Mohsen Amini[a,b]*

[a]Department of Medicinal Chemistry, Faculty of Pharmacy, Tehran University of Medical Sciences, Tehran14176, Iran. email: moamini@tums.ac.ir; barazand@tums.ac.ir

[b]The Institute of Pharmaceutical Sciences (TIPS), Tehran University of Medical Sciences, Tehran, Iran

[c]Department of Pharmacology and Toxicology, Faculty of Pharmacy, Tehran University of Medical Sciences, Tehran14176, Iran

Abstract – The aim of this study is synthesis of new diarylimidazole-quinazolinone hybrid derivatives to target two binding sites of tubulin, an attractive target for design of anticancer drugs. In this report, the location of the accessible space of active site was determined by comparing the crystal structure of different inhibitors in tubulin structure. The docking and molecular dynamic simulations were used to confirm the position and stability of designed compounds. Thirteen new compounds were synthesized and their cytotoxicity were studied on three types of cancerous cell lines. Some of the synthesized compounds showed remarkable anti-proliferative activity in cell culture study.

INTRODUCTION

Microtubule plays an important role in maintaining the structure of eukaryotic cell, as well as in the process of transmission and reproduction of the cell, so it is an attractive target for design of anticancer drugs.[1, 2] α- and β-Tubulin heterodimers are head-to-head interconnected, and make protofilaments. Microtubule is a result of side by side connection of the protofilaments.[3] A wide range of molecules can bind tubulin and changes its dynamic. After approval of vincristine in 1963, the study continues on molecules affecting tubulin. Five drug-binding sites were identified on tubulin, including taxane, vinca alkaloid, colchicine, laulimalide, and maytansine.[4-9] Many anti-tubulin molecules designed to target these sites. Among that,

most of inhibitors have been design to target colchicine-binding site, but no drug of this mechanism has been approved for cancer treatment.

Colchicine was firstly extracted from the leaf of Meadow Saffron (*Colchicum autumnale*) and used to treat gout.[11] In 1968, colchicine binding site was located and then colchicine structure and its mechanism of action have been identified.[7,12-15] These compounds cause the stability of the curved structure by connecting to the β subunit of a tubulin, so repulsion with α subunit, prevent them from redecoration in the form of direct structure, and reformation of the tubulin subunits.[13] Dong et al. reviewed a series of chemically diverse natural and synthetic compounds and presented at least four different categories of compound with different SAR.[16] This study revealed that very different structures can occupied the colchicine binding site and inhibited tubulin polymerization. Crystal structure of tubulin in the presence of small molecule inhibitor revealed that they often occupied two major spaces next to each other.[17] Since colchicine binding site has a large area, inhibitors with different structures and conformations can locate in this space, making difficult recognition of correct conformation through docking simulation. In this study, we superimposed over 50 crystal structures of tubulin in the presence of inhibitors to locate the detailed accessible area in the colchicine binding site. Then we selected Lexibulin-binded as a most expanded structure to use in docking simulation. Design of new structure has been done so that they can fill most of accessible spaces.

Several natural quinazolin-4-one derivatives have been recognized with potential anticancer activity. For example bouchardantine, 2-substituted quinazolinin-4-one alkaloids (Figure 1, a) showed a remarkable anticancer activity.[18] Furthermore, the synthesized quinazolinin-2-one derivatives bearing *trans*-stilbene (Figure 1, b) moiety demonstrated anti-proliferative properties against some cancerous cell line including MCF-7, T47D.[19] A hybrid of quinazolinone and thiadiazole-urea with a thiomethyl spacer (Figure 1, c) was reported as anti-proliferative agents.[20]

On the other hand, the anticancer activity of diarylheterocyclic compounds such as diarylimidazolyl and diarylthiozolyl derivatives (Figure 1, d) were studied as anticancer agent with inhibition of tubulin as mechanism of action.[21,22,24,25] Some of them showed potent activity for inhibition of breast cancerous cell line. In the current work, we report design and synthesis of a novel combination of two moieties groups (Figure 1, e), quinazolin-4-one and diarylimidazole and evaluation of their cytotoxicity properties.

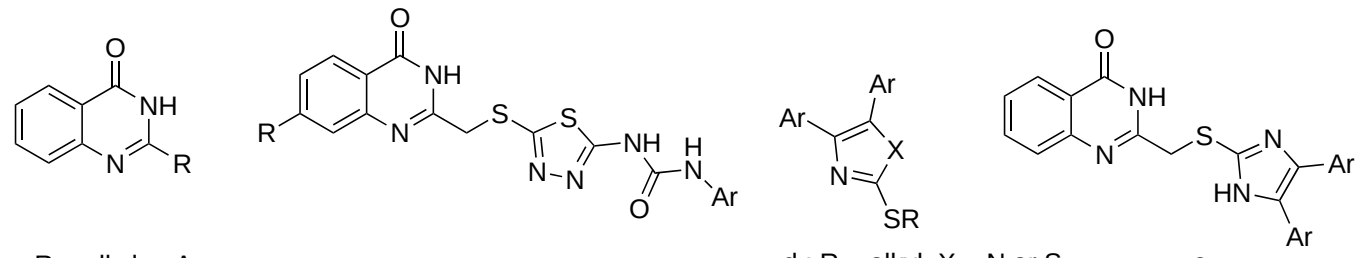

Figure 1. Structure of quinazolin-4-one and diarylimidazole or thiazole derivatives with anti-cancer activity

RESULTS AND DISCUSSION

All compounds were synthesized as shown in Scheme 1. Diarylbenzoin derivatives **2** were prepared through benzoin condensation as the reported procedure.[21] Imidazole-2-thione derivatives **3** were prepared from reaction of the different benzoin with ammonium thiocyanate in presence of thiourea in *n*-butanol under reflux condition for 15 h. Our experiments showed that the ratio of ammonium thiocyanate and thiourea is important in yields of the reaction. The optimum ratio (3:1) was used for the preparation of compound **3**. Synthesis of quinazolinone derivatives **5** was carried out as the previously reported method.[23] Compounds **6a-j** were prepared from S_N2 reaction of imidazole-2-thione derivatives **3** and different quinazolinones **5** in methanol as the solvent and the presence of small amounts of triethylamine. Oxidation of sulfur atom in compound **6** was carried out by oxone in methanol for conversion to the related of sulfinyl derivatives **7**. The purity of the synthesized compounds was checked by HPLC using a reversed phase HPLC system and UV detection at 285 nm in concentration of 300 µg/mL for all compounds. The mobile phase contain MeCN : MeOH : H_2O : HOAc with different compositions (22 : 37 : 40 : 1, mobile phase A ; 40 : 19 : 40 : 1, mobile phase B) were used for analysis of **6a-j** and **7a-c**. The separation was performed on a C18 column (25 cm, 5 µm *id*). The purity of the test compounds is presented in Table 1.

Docking study

To consider detailed space of active site, all crystal structures of tubulin in complex with small molecule inhibitors were retrieved from the RCSB protein data bank. Over 50 structures were superimposed over each other to probe accessible spaces in active site. Study of different crystal structures revealed that the colchicine binding site is very flexible and can cause new space to be open in the presence of some ligands. Nocodazole and plinabulin are examples of ligands occupied narrow space which are not present in Apo state of tubulin.[13] Crystalline structure of tubulin in complex with nocodazole or plinabulin revealed that occupation of this active site shrinks colchicine-binding site so that docking simulation cannot pose colchicine in correct position.

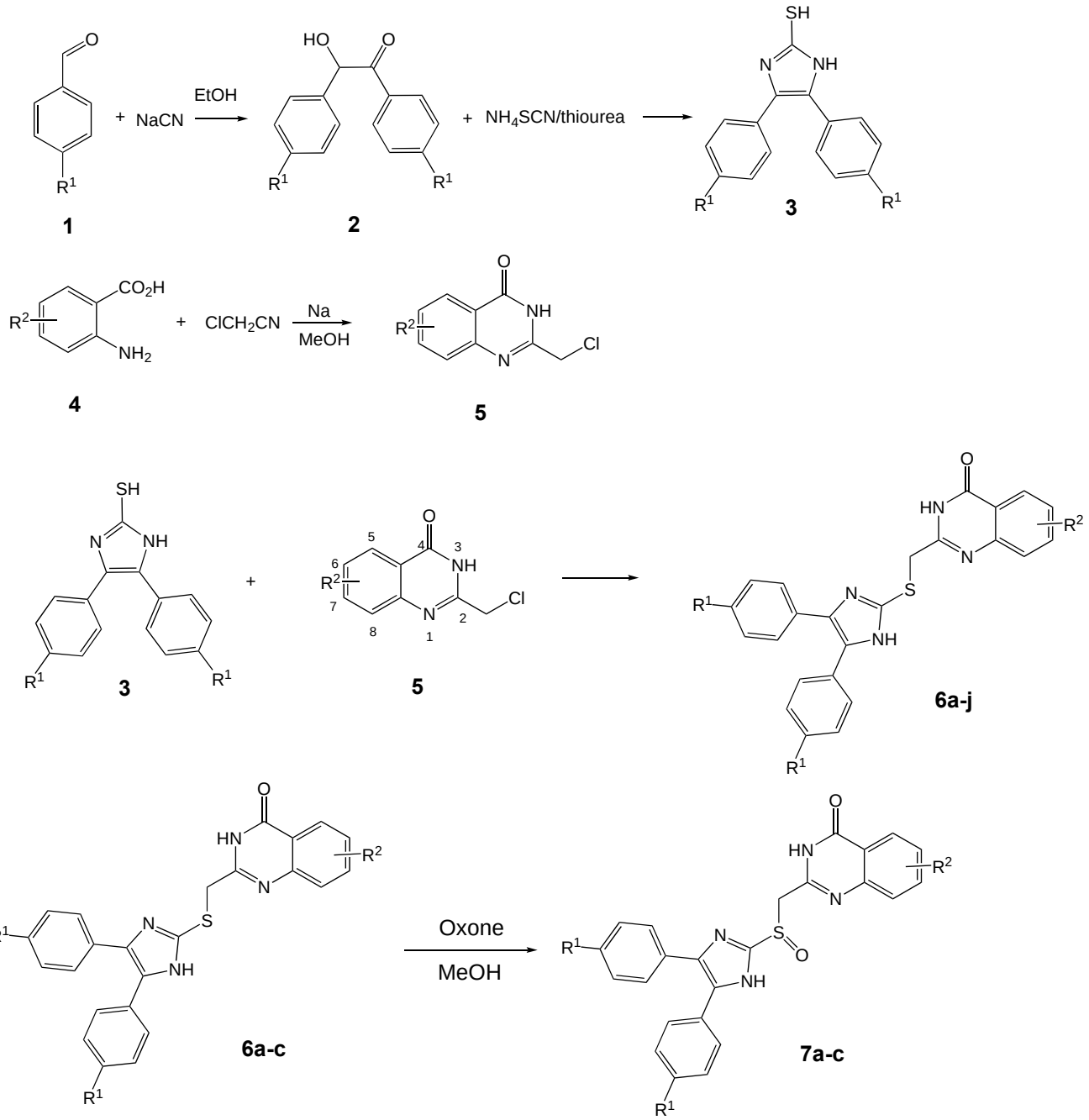

R^1 = H, Me, OMe, F, SMe, Cl
R^2 = H, 6-Me, 6-Cl, 6,7-*di*OMe

6a: R^1, R^2 = H; **6b**: R^1 = H, R^2 = 6-Me; **6c**: R^1 = H, R^2 =6 -Cl; **6d**: R^1 = H, R^2 = 6,7-dimethoxy; **6e**: R^1 = Me, R^2 = H; **6f**: R^1 = OMe, R^2 = 6,7-dimethoxy; **6g**: R^1 = Me, R^2 = 6,7-dimethoxy; **6h**: R^1 = F, R^2 = 6,7-dimethoxy; **6i**: R^1 = SMe, R^2 = 6,7-dimethoxy; **6j**: R^1 = Cl, R^2 = 6,7-dimethoxy; **7a**: R^1, R^2 = H; **7b**: R^1 = H, R^2 = 6-Cl; **7c**: R^1 = H, R^2 = 6-Me

Scheme 1. The synthesis pathway for preparation of compounds **6** and **7**

Table 1. The purity of compounds **6a-j** and **7a-c**, checked by HPLC

Name	Mobile Phase	Flow Rate (mL/min)	Retention Time (min)	Purity (%)
6a	A	1	13.90	99.51
6b	B	1	9.35	98.36
6c	B	1	14.93	98.02
6d	A	1.5	7.79	99.35
6e	B	1	12.10	98.86
6f	B	1	6.06	98.82
6g	B	1.5	8.39	99.16
6h	B	1	5.23	99.32
6i	B	1	20.09	98.56
6j	B	1.5	26.53	98.68
7a	A	1	12.44	99.18
7b	B	1	10.24	98.72
7c	A	1.5	10.94	98.8

Therefore, we selected the most expanded crystalline structure to use in docking simulation. Since lexibuline bonded tubulin structure (5CA0) has enough space in both colchicine and nocodazole binding site, it is suitable structure for docking simulation. In our previous research, we designed some diaryl-imidazole derivatives, which occupied colchicine-binding site.[20] To improve potency, we designed some hybrid small molecules to occupy both colchicine and nocodazole binding site. Quinazolin-4(3*H*)-one was selected as a scaffold to fill nocodazole binding site and attached to imidazole ring by thiomethyl linkage. The rotation of linkage provides needed flexibility to adjust molecule with the curvature of binding site. Quinazolin-4(3*H*)-one derivatives revealed anti-proliferative, anti-angiogenic, and anticancer activity.[21,23] Molecular modeling study was performed in order to investigate the binding interaction of the synthesized compounds on colchicine binding site of tubulin. Molecular docking was done on tubulin structure (PDB code: 5CA0) using induce fit and genetic algorithm to determine the proper conformation of compounds in the colchicine binding site. Docking simulation revealed that the best interaction will be done by 4,5-dimethoxy derivative of quinazolinone.

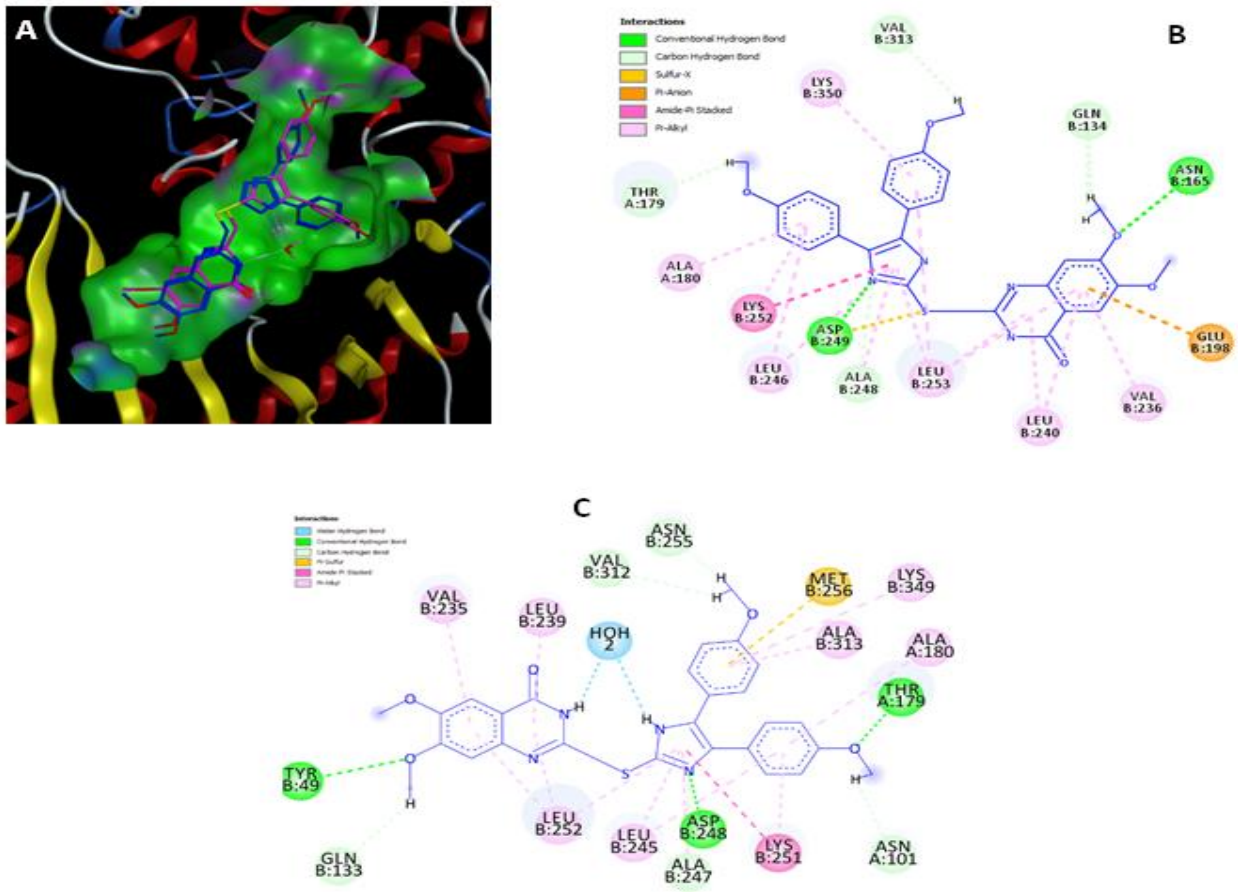

Figure 2. Position of **6f** in active site before and after of molecular dynamic and their interactions

Representation of **6f** pose in the active site (A) after docking simulation (red) in compare with occupied position after molecular dynamic simulation (blue). Molecule changed its position to become more stable in active site through making new interaction. Comparison of ligand interactions before (B) and after (C) molecular dynamic simulation revealed that molecule was success to make new hydrogen bond with ASP 248 and TYR 49 and THR 179 from Colchicine binding site. Also, there is enough space to be occupied by one water molecule which made hydrogen bond with imidazole and quinazolin moieties.

Dynamic study

MD simulation was performed in NAMD using explicit solvent model and Amber10 force field to parameterize protein and ligand. Explicit water molecule simulation was performed to study water molecule interaction in complex with ligand and receptor. The trajectory was analyzed using VMD 1.9.0 software, and discovery studio 4.5 was used to reveal 2D interaction.

Molecular dynamic simulation using NAMD was applied to study the stability of ligand in the active site. Moreover, we used molecular dynamic to determine the flexibility tubulin and the position of water

molecule. We had assumed that strongly interaction of inhibitor with colchicine binding site would reduce its flexibility and changed its function.

Analysis of trajectory revealed tubulin dynamic changes in complex with ligands and in Apo structure during 50 ns simulation (Figure 2). The results show that binding of **6f** decreases tubulin flexibility in the 50 ns period, which plays an important role in inhibiting the polymerization of tubulin. Also, the molecular dynamic shows the ligand stability in colchicine binding site. RMSD fluctuation in acceptable range show the stability of **6f** in colchicine binding site. After 30 ns molecular dynamic simulation, ligand became stable in active cite and made strong interaction with key amino acids (ASP 249, LEU 253, GLU198, ASN 165) through hydrogen bonding. Moreover, there is a position to be occupied by a molecule of water in the active site which made hydrogen bond with both imidazole and quinazoline nitrogen atoms. RMSD fluctuation vs time revealed that ligand was stable in the active site during simulation and able to reduce tubulin flexibility which is important in its polymerization (Figure 3).

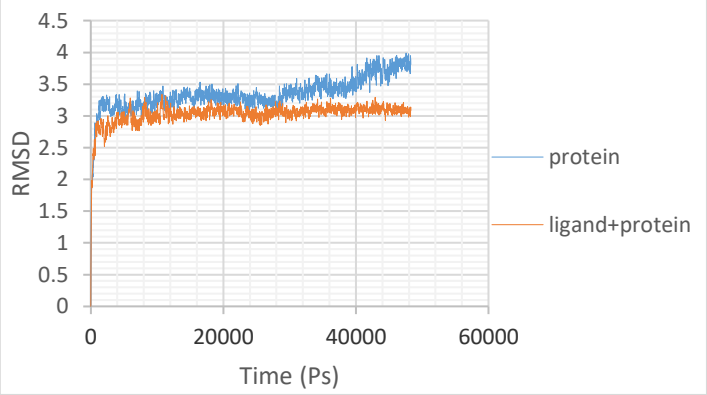

Figure 3. RMSD vs time in 50 ns molecular dynamic simulation

Protein flexibility has been reduced in the presence of ligand in compare with apo structure. As can be seen, after 30 ns the flexibility of apo protein gradually increased to the end of simulation.

Biological study

Cytotoxicity Evaluation by MTT Assay

The cytotoxic effects of the synthesized compounds were evaluated against human colon adenocarcinoma (HT-29), two breast cancer cell lines (MCF-7 and T47D), as well as a mouse embryonic fibroblast normal cell line, NIH-3T3, by the MTT assay. Paclitaxel was used as positive control. Ability of inhibiting cell growth has been presented in Table 2 as IC_{50} value. Compound **6c** has shown the best cytotoxic activity against MCF-7 (15 μM). The most cytotoxic activities against HT-29 and T47D were observed by compounds **6g** and **6f** respectively. According to Table 2, it seems that oxidation of sulfur atom to S-oxide group **7a-c** decreases the activity in all cell lines. It is interesting to point, in case of **6f** the remarkable

selectivity was observed in comparison of the cytotoxicity effect between T47D and normal cell lines (NIH3T3). Altogether, according to the IC_{50} of the test compounds, it seems beneficial to investigate other derivatives of diarylimidazole-quinazolinone scaffold for finding more potent and safer anticancer agents.

Table 2. In vitro cytotoxic activities (IC_{50}) of compounds **6a-j** and **7a-c**

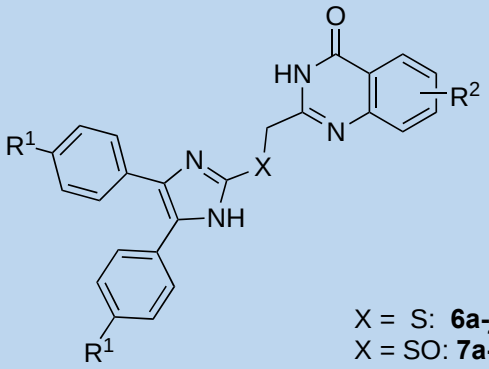

Compounds	R^1	R^2	HT-29	T47D	MCF7	NIH3T3
6a	H	H	34.48±3.13	41.76±0.94	53.9±1.88	57.86±6.94
6b	H	6-Me	48.75±0.76	38.30±0.30	29.88±1.16	35.19±2.63
6c	H	6-Cl	29.59±2.01	29.32±2.05	15.63±2.98	20.93±0.46
6d	H	6,7-OMe	57.46±0.94	61.37±3.46	63.07±6.98	60.14±12.36
6e	Me	H	>100	34.48±6.32	29.43±2.94	90.03±11.76
6f	OMe	6,7-OMe	30.76±0.84	**5.98±0.45**	61.29±4.12	70.21±9.98
6g	Me	6,7-OMe	23.5±3.14	**6.75±1.99**	27.01±1.67	24.89±0.14
6h	F	6,7-OMe	39.23±1.02	61.37±4.42	51.61±1.23	50.67±3.02
6i	SMe	6,7-OMe	63.68±0.98	>100	39.9±0.23	21.76±1.2
6j	Cl	6,7-OMe	30.14±1.25	27.39±2.97	33.05±6.28	27.95±5.13
7a	H	H	>100	>100	>100	134.25±15.14
7b	H	6-Cl	>100	85.03±11.20	>100	77.26±2.69
7c	H	6-Me	72.84±6.78	70.03±2.99	>100	66.19±1.88
Paclitaxel			5.43±1.20	>100	44.21±3.20	2.19±0.29

EXPERIMENTAL

General

^{1}H and ^{13}C NMR spectra were recorded with a Varian FT-500, using TMS as an internal standard. Coupling constant (*J*) values are presented in hertz (Hz) and spin multiples are given as s (singlet), d (double), t (triple), and m (multiple). Melting points were determined with a Kofler hot stage apparatus and are uncorrected. Infrared spectra were acquired on a Nicolet Magna 550-FT spectrometer. IR spectra of solid were recorded in KBr and the absorption band was given in wave numbers in cm^{-1}. Melting points were determined with a Kofler hot stage apparatus and are uncorrected. Mass spectra were obtained with an Agilent Technology (HP) mass spectrometer operating at an ionization potential of 70 eV. Elemental analyses for C, H, and N were determined with an Elementar Analysen System GmbH VarioEL CHN mode.

Chemistry

General procedure for the synthesis of benzoin derivatives 2

To 71.2 mmol of the related benzaldehydes, were added 25 mL of EtOH, 5 mL of H_2O and 1 g of NaCN in a 100 mL round bottom flask. The mixture was stirred for 24 h at rt. The mixture of reaction was filtered and the precipitate was washed with H_2O and cold EtOH. The curd product was crystalized in MeOH.

General procedure for the synthesis of diarylimidazoles 3

The different diarylimidazole derivatives **3** were synthesized as the reported procedure.[21] The related benzoin (20 mmol) was dissolved in 50 mL of *n*-BuOH, 4.6 g of NH_4SCN (60 mmol) and 1.5 g of thiourea (23 mmol) were added to the solution. The reaction mixture was refluxed for 15 h. After cooling to the rt, H_2O was added to the solution and then filtered. The solid precipitate was crystalized in CH_2Cl_2 to give the pure diarylimidazole derivatives.

General procedure for the synthesis of 4(3*H*)-quinazolinone derivatives 5

4(3*H*)-Quinazolinone derivatives were prepared as the literature procedure.[23] Na (115 mg) was dissolved in 25 mL of dry MeOH and a solution of 4.75 mL of (75 mmol) $ClCH_2CN$ in 50 mL of dry MeOH was added to the solution by dropping funnel in 20 min. Anthranilic acid derivatives (25.6 mmol) in 75 mL of dry MeOH were added to the mixture and left to stirrer at rt for 4 h. Then the solid was filtered and washed with cold MeOH three times to give the related pure quinazolinones.

General procedure for the synthesis of 6a-j

The compounds **6a-j** were synthesized from condensation of diarylimidazole and quinazolinone derivatives. Diaryllimidazole (3 mmol) was dissolved in 50 mL of MeOH and 0.75 mL of Et_3N was added to the solution.

The reaction temperature was raised to boiling temperature and a solution of the related quinazolinone (3 mmol) in 5 mL of MeOH was added to the reaction mixture and stirred for 10 h. The solvent was distilled under vacuum and the solid precipitate was washed with H_2O and EtOAc to give **6a-j**.

2-(((4,5-Diphenyl-1*H*-imidazol-2yl)thio)methyl)quinazolin-4(3*H*)-one 6a

Yield 80%, white solid, mp 245-247 °C, IR KBr, 623, 693, 754, 782, 846, 1073, 1186, 1251, 1311, 1365, 1445, 1492, 1515, 1565, 2960 cm^{-1}. ^1H NMR (DMSO-d_6, 500 MHz) δ: 12.99 (s, 1H, NH), 12.84 (s, 1H, NH), 8.13 (d, *J* = 7.7 Hz, 1H), 7.78 (t, *J* = 7.2 Hz, 1H), 7.59 (d, *J* = 8.0 Hz, 1H), 7.20-7-52 (m, 11H), 4.29 (s, 2H, CH_2). ^{13}C NMR (DMSO-d_6, 125 MHz) δ: 161.62, 154.27, 148.54, 139.24, 137.24, 134.43, 130.47, 128.68, 128.27, 127.87, 126.98, 126.63, 125.82, 121.20, 36.66. MS, *m/z* (%): 410 (10), 377 (15), 252 (100), 218 (20), 193 (45), 165 (42), 104 (26), 77 (25). Anal. Calcd for $C_{24}H_{18}N_4OS$: C, 70.22; H, 4.42; N, 13.65. Found: C, 70.11; H, 4.27; N, 13.29.

6-Methyl-2-(((4,5-diphenyl-1*H*-imidazol-2-yl)thio)methyl)quinazolin-4(3*H*)-one 6b

Yield 85%, white solid, mp 235-237 °C IR KBr, 407, 512, 622, 651, 693, 754, 782, 822, 844, 1019, 1082, 1185, 1249, 1288, 1310, 1365, 1440, 1490, 1515, 1566, 2938, 3062 cm^{-1}. ^1H NMR (DMSO-d_6, 500 MHz) δ: 12.92 (s, 1H, NH), 12.85 (s, 1H, NH), 7.93 (s, 1H), 7.59 (d, *J* = 7.8 Hz, 1H), 7.46- 7.58 (m, 2H), 7.10-7.40 (m, 9H), 4.28 (s, 2H, CH_2), 2.43 (s, 3H, CH_3). ^{13}C NMR (DMSO-d_6, 125 MHz) δ 161.53, 153.32, 146.52, 139.40, 137.21, 136.33, 135.64, 134.35, 130.49, 128.67, 128.25, 127.92, 127.59, 127.05, 126.85, 125.23, 120.95, 36.57, 20.80. MS, *m/z* (%): 424 (70), 391 (100), 252 (30), 193(82), 104 (15), 77 (15). Anal. Calcd for $C_{25}H_{20}N_4OS$: C, 70.73; H, 4.75; N, 13.20. Found: C, 70.94; H; 4.91; N, 12.94.

6-Chloro-2-(((4,5-diphenyl-1*H*-imidazol-2-yl)thio)methyl)quinazolin-4(3*H*)-one 6c

Yield 85%, white solid, mp 245-247 °C, IR KBr, 476, 624, 684, 749, 779, 819, 842, 1023, 1071, 1185, 1234, 1309, 1363, 1434, 1493, 1518, 1567, 2940 cm^{-1}. ^1H NMR (DMSO-d_6, 500 MHz) δ: 13.09 (s, 1H, NH), 12.83 (s, 1H, NH), 8.11 (d, *J* = 8.5 Hz, 1H), 7.61 (s, 1H), 7.18-7.52 (m, 11H), 4.25 (s, 2H, CH_2). ^{13}C NMR (DMSO-d_6, 125 MHz) δ: 161.04, 155.90, 149.65, 139.03, 138.84, 137.31, 134.31, 130.45, 129.13, 128.70, 128.66, 128.25, 128.22, 128.08, 127.92, 127.87, 127.58, 127.01, 126.98, 126.86, 126.16, 124.71, 120.03, 36.75. MS, *m/z* (%): 446 (17), 444 (50), 411 (65), 252 (100), 219 (40), 193 (90), 165 (60), 104 (25), 77(26). Anal. Calcd for $C_{24}H_{17}ClN_4OS$: C, 64.79; H, 3.85; N, 12.59. Found: C, 64.91; H, 4.05; N, 12.29.

6,7-Dimethoxy-2-(((4,5-diphenyl-1*H*-imidazol-2-yl)thio)methyl)quinazolin-4(3*H*)-one 6d

Yield 85%, white solid, mp 245-248 °C IR KBr, 407, 512, 622, 651, 693, 754, 782, 822, 844, 1019, 1082, 1185, 1249, 1288, 1310, 1365, 1440, 1490, 1515, 1566, 2938, 3062 cm-1. ^1H NMR (DMSO-d_6, 500 MHz)

δ: 12.83 (brs, 2H, NH), 7.10-7.51 (m, 13H), 7.04 (s, 1H), 4.25 (s, 2H, CH_2), 3.86 (s, 3H, OCH_3), 3.84 (s, 3H, OCH_3). ^{13}C NMR (DMSO-*d*$_6$, 125 MHz) δ: 161.39, 154.98, 153.03, 148.97, 144.98, 139.90, 129.15, 129.12, 128.72, 128.69, 128.36, 128.34, 127.52, 127.49, 114.56, 108.29, 105.46, 56.32, 56.14, 36.94. MS, *m/z* (%): 470 (70), 437 (100), 252 (20), 220 (20), 193 (55), 165 (15) Anal. Calcd for $C_{26}H_{22}N_4O_3S$: C, 66.37; H, 4.71; N, 11.91. Found: C, 66.49; H, 4.87; N, 11.62.

2-(((4,5-Di-*p*-tolyl-1*H*-imidazol-2-yl)thio)methyl)quinazolin-4(3*H*)-one 6e

Yield 80%, white solid, mp 240-242 °C, IR KBr, 464, 513, 563, 578, 637, 691, 760, 827, 1018, 1072, 1111, 1173, 1235, 1257, 1308, 1372, 1414, 1453, 1506, 1569, 1609, 1741, 2846, 2922 cm^{-1}. ^{1}H NMR (DMSO-*d*$_6$, 500 MHz) δ: 13.04 (s, 1H, NH), 12.74 (s, 1H, NH), 8.14 (d, *J* = 7.8 Hz, 1H), 7.70-7.80 (m, 1H), 7.55-7.60 (m, 1H), 7.501-7.53 (m, 2H), 7.08-7.49 (m, 7H), 4.26 (s, 2H, CH_2), 2.31 (s, 3H, CH_3), 2.28 (s, 3H, CH3). ^{13}C NMR (Dmso-*d*$_6$, 125 MHz) δ: 161.59, 154.34, 148.53, 138.82, 137.17, 137.01, 135.84, 134.43, 134.20, 131.59, 129.26, 128.83, 127.73, 126.99, 126.86, 126.63, 126.32, 125.82, 125.62, 121.20, 36.69, 20.77. MS, *m/z* (%): 438 (60), 405 (100), 280 (12), 221 (45), 160 (13). Anal. Calcd for $C_{26}H_{22}N_4OS$: C, 71.21; H, 5.06; N, 12.78. Found: C, 71.03; H, 5.20; N, 12.99.

6,7-Dimethoxy-2-(((4,5-bis(4-methoxyphenyl)-1*H*-imidazol-2-yl)thio)methyl)quinazolin-4(3*H*)-one 6f

Yield 85%, white solid, mp 245-247 °C, IR KBr, 500, 581, 637, 693, 729, 764, 827, 848, 1016, 1086, 1110, 1172, 1236, 1258, 1308, 1374, 1410, 1455, 1569, 1606, 2916 cm-1. ^{1}H NMR (DMSO-*d*$_6$, 500 MHz) δ: 12.98 (s, 1H, NH), 12.67 (s, 1H, NH), 7.46 (s, 3H), 7.31 (d, *J* = 7.3 Hz, 2H), 7.06 (s, 1H), 6.97 (d, *J* = 7.2 Hz, 2H), 6.86 (d, *J* = 7.6 Hz, 2H), 4.23 (s, 2H, CH_2), 3.88 (s, 3H, OCH_3), 3.87 (s, 3H, OCH_3), 3.78 (s, 3H, OCH_3), 3.75 (s, 3H, OCH_3). ^{13}C NMR (DMSO-*d*$_6$, 125 MHz) δ: 160.94, 158.82, 158.07, 154.54, 152.75, 148.52, 144.54, 138.57, 136.44, 129.25, 128.14, 127.90, 126.96, 122.92, 114.16, 114.11, 113.68, 107.86, 105.01, 55.89, 55.70, 55.17, 55.02, 36.56. MS, *m/z* (%): 530 (40), 497 (95), 312 (100), 253 (75), 220 (30). Anal. Calcd for $C_{28}H_{26}N_4O_5S$: C, 63.38; H, 4.94; N, 10.56. Found: C, 63.47; H, 5.11; N, 10.41.

6,7-Dimethoxy-2-(((4,5-di-*p*-tolyl-1*H*-imidazol-2-yl)thio)methyl)quinazolin-4(3*H*)-one 6g

Yield 85%, white solid, mp 248-250 °C, IR KBr, 524, 583, 638, 692, 730, 762, 829, 848, 1018, 1076, 1175, 1239, 1262, 1309, 1374, 1415, 1456, 1508, 1570, 1579, 1609, 2846, 2917 cm^{-1}. ^{1}H NMR (DMSO-*d*$_6$, 500 MHz) δ: 12.89 (s, 1H, NH), 12.74 (s, 1H, NH), 7.45 (s, 1H), 7.42 (d, *J* = 7.3 Hz, 2H), 7.28 (d, *J* = 7.2 Hz, 2H), 7.19 (d, *J* = 7.3 Hz, 2H), 7.09 (d, *J* = 7.4 Hz, 2H), 7.05 (s, 1H), 4.24 (s, 2H, CH_2), 3.87 (s, 3H, OCH_3), 3.85 (s, 3H, OCH_3), 2.31(s, 3H, CH_3), 2.27 (s, 3H, CH_3). ^{13}C NMR (DMSO-*d*$_6$, 125 MHz) δ: 160.92, 154.53, 152.68, 148.52, 144.53, 139.03, 137.18, 136.96, 135.84, 131.60, 129.26, 128.81, 128.59, 127.71, 126.95,

114.11, 107.84, 105.01, 55.87, 55.69, 36.52, 20.79, 20.78. MS, *m/z* (%): 498 (60), 465 (100), 280 (20), 221 (50). Anal. Calcd for $C_{28}H_{26}N_4O_3S$: C, 67.45; H, 5.26; N, 11.24. Found: C, 67.65; H, 5.34; N, 11.03.

2-(((4,5-Bis(4-fluorophenyl)-1*H*-imidazol-2-yl)thio)methyl-6,7-dimethoxyquinazolin-4(3*H*)-one 6h

Yield 81%, solid, mp 218-220 °C, IR KBr, 463, 522, 582, 637, 692, 726, 762, 806, 827, 848, 1018, 1075, 1110, 1173, 1236, 1258, 1309, 1372, 1413, 1454, 1510, 1569, 1609 cm^{-1}. ^1H NMR (DMSO-d_6, 500 MHz) δ: 12.78 (brs, 2H, NH), 7.25-7.44 (m, 5H), 7.00-7.17 (m, 6H), 4.25 (s, 2H, CH_2), 3.87 (s, 3H, OCH_3), 3.86 (s, 3H, OCH_3). ^{13}C NMR (DMSO-d_6, 125 MHz) δ: 161.95 (d, J_{CF} = 247.4 Hz), 160.83, 154.63, 154.56, 152.48, 150.63, 148.96, 148.54, 144.56, 139.42, 130.18, 128.96, 115.40 (J_{CF} = 33.7 Hz), 114.09, 108.16, 107.84, 104.96, 55.89, 55.70, 36.47. MS, *m/z* (%): 506 (25), 473 (45), 304(35), 288 (100), 229 (70), 220 (50), 201 (35), 122(30). Anal. Calcd for $C_{26}H_{20}F_2N_4O_3S$: C, 61.65; H, 3.98; N, 11.06. Found: C, 61.50; H, 3.84; N, 11.19.

6,7-Dimethoxy-2-(((4,5-bis(4-(methylthio)phenyl)-1*H*-imidazol-2-yl)thio)methyl)quinazolin-4(3*H*)-one 6i

Yield 80%, white solid, mp 238-240 °C, IR KBr, 465, 573, 636, 694, 756, 777, 822, 846, 1023, 1071, 1181, 1238, 1293, 1365, 1404, 1448, 1510, 1570, 1606, 3029 cm^{-1}. ^1H NMR (DMSO-d_6, 500 MHz) δ: 12.85 (brs, 2H, NH), 7.97 (s, 1H), 7.07-7.47 (m, 9H), 4.27 (s, 2H, CH_2), 3.89 (s, 3H, OCH_3), 3.88 (s, 3H, OCH_3) 2.90 (s, 3H, SCH_3), 2.75 (s, 3H, SCH_3). ^{13}C NMR (DMSO-d_6, 125 MHz) δ: 162.28, 160.91, 154.54, 152.58, 148.53, 144.52, 139.41, 136.51, 130.98, 128.26, 127.47, 125.80, 114.09, 107.84, 105.00, 55.89, 55.70, 36.46, 14.50. MS *m/z* (%): 562 (1), 436 (20), 254(21), 220 (100), 205 (30), 86 (80), Anal. Calcd for $C_{26}H_{20}N_4O_3S$: C, 59.76; H, 4.66; N, 9.96. Found: C, 59.88; H, 4.81; N, 9.81.

2-(((4,5-Bis(4-chlorophenyl)-1*H*-imidazol-2-yl)thio)methyl)-6,7-dimethoxyquinazolin-4(3*H*)-one 6j

Yield 86%, white solid, mp 227-230 °C, IR KBr, 406, 495, 520, 590, 639, 665, 719, 744, 782, 819, 837, 900, 982, 1013, 1090, 1156, 1189, 1225, 1268, 1297, 1329, 1408, 1429, 1490, 1563, 1603, 1661, 1911, 2968, 3073 cm^{-1}. ^1H NMR (DMSO-d_6, 500 MHz) δ: 12.94 (s, 1H, NH), 12.69 (s, 1H, NH), 7.00-7.5 (m, 10H), 4.26 (s, 2H, CH_2), 3.87 (s, 3H, OCH_3), 3.85 (s, 3H, OCH_3). ^{13}C NMR (DMSO-d_6, 125 MHz) δ: 160.90, 154.55, 152.37, 148.53, 144.52, 140.01, 129.54, 128.76, 128.62, 114.06, 107.83, 104.99, 55.90, 55.71, 36.39. MS, *m/z* (%): 538 (40), 505 (65), 320 (60), 220 (50), 158 (70), 139 (100), 112 (65), 82 (65). Anal. Calcd for $C_{26}H_{20}Cl_2N_4O_3S$: C, 57.89; H, 3.74; N, 10.39. Found: C, 58.04; H, 3.91; N, 10.16.

General procedure for the synthesis of 7a-c

Oxone as oxidizer reagent was used for oxidation of sulfur atom to S-oxide group. A solution of 0.92 g (1.5 mmol) of oxone in 10 mL of H_2O was added to a solution of the compound **6** (1 mmol) in 20 mL of MeOH. The mixture was stirred at rt overnight. The participated was filtered and crystallized in EtOAc.

2-(((4,5-Diphenyl-1*H*-imidazol-2yl)sulfinyl)methyl)quinazolin-4(3*H*)-one 7a

Yield 89%, white solid, mp 227-229 °C, IR KBr, 472, 524, 574, 635, 691, 724, 757, 779, 823, 847, 1018, 1071, 1093, 1152, 1187, 1237, 1294, 1311, 1365, 1417, 1444, 1508, 1568, 1600, 2856 cm^{-1}. ^1H NMR (DMSO-d_6, 500 MHz) δ: 13.79 (s, 1H, NH), 12.56 (s, 1H, NH), 8.10 (d, *J* = 7.6 Hz, 1H), 7.80 (t, *J* = 7.75 Hz, 1H), 7.25-7.65 (m, 12H), 4.78 (d, *J* = 13.3 Hz, 1H, CH_2), 4.67 (d, *J* = 13.3 Hz, 1H, CH_2). ^{13}C NMR (DMSO-d_6, 125 MHz) δ: 161.33, 148.88, 148.35, 145.90, 137.89, 134.57, 134.01, 130.58, 129.86, 128.76, 128.74, 128.38, 128.30, 127.22, 126.97, 126.87, 125.82, 121.11, 57.71. MS, *m/z* (%): 406 (10), 378 (20), 252 (100), 220 (90), 193 (25), 165 (60). Anal. Calcd for $C_{24}H_{18}N_4O_2S$: C, 67.59; H, 4.25; N, 13.14. Found: C, 67.81; H, 4.34; N, 12.97.

6-Chloro-2-(((4,5-diphenyl-1*H*-imidazol-2-yl)sulfinyl)methyl)quinazolin-4(3*H*)-one 7b

Yield 75%, white solid, mp 220-223 °C, IR KBr, 407, 483, 525, 574, 640, 685, 757, 819, 847, 1025, 1071, 1101, 1185, 1240, 1313, 1363, 1446, 1513, 1563, 1606, 2920 cm^{-1}. ^1H NMR (DMSO-d_6, 500 MHz,) δ: 13.80 (s, 1H, NH), 12.71 (s, 1H, NH), 8.09 (d, *J* = 8.5 Hz, 1H), 7.20-7.65 (m, 12H), 4.77 (d, *J* = 13.3 Hz, 1H, CH_2), 4.66 (d, *J* = 13.3, 1H, CH_2). ^{13}C NMR (DMSO-d_6, 125 MHz) δ: 160.73, 150.52, 149.43, 145.73, 139.16, 137.96, 134.01, 130.63, 129.83, 128.68, 128.39, 127.91, 127.57, 127.26, 127.10, 126.15, 119.94, 57.88. MS, *m/z* (%): 252 (90), 220 (100), 194 (80), 165 (75), 124 (30), 64 (45). Anal. Calcd for $C_{24}H_{17}ClN_4O_2S$: C, 62.54; H, 3.72; N, 12.16. Found: C, 62.46; H, 3.65; N, 12.29.

6-Methyl-2-(((4,5-diphenyl-1*H*-imidazol-2-yl)sulfinyl)methylquinazolin-4(3*H*)-one (7c)

Yield 85%, white solid, mp 230-232 °C, IR KBr, 496, 573, 736, 766, 828, 1010, 1069, 1091, 1154, 1232, 1309, 1364, 1401, 1516, 1573, 1599, 1899, 2928, 2980, 3059 cm^{-1}. ^1HNMR (DMSO-d_6, 500 MHz,) δ: 13.82 (s, 1H, NH), 12.50 (s, 1H, NH), 7.93 (s, 1H), 7.63 (d, *J* = 8.2 Hz, 1H), 7.51 (d, *J* = 8.2 Hz, 1H), 7.27-7.44 (m, 10H), 4.81 (d, *J* = 13.4 Hz, 1H, CH_2), 4.68 (d, *J* = 13.4 Hz, 1H, CH_2), 2.45 (s, 3H, CH_3). ^{13}C NMR (DMSO-d_6, 125 MHz) δ: 161.27, 147.94, 146.39, 145.95, 137.89, 136.62, 135.78, 134.01, 130.60, 129.87, 128.75, 128.72, 128.43, 128.38, 128.30, 127.26, 127.22, 126.84, 125.19, 120.88, 57.70, 20.81. MS, *m/z* (%): 420 (5), 392 (10), 252 (100), 219 (55), 193 (35), 165 (60). Anal. Calcd for $C_{25}H_{20}N_4O_2S$: C, 68.16; H, 4.58; N, 12.72. Found: C, 68.23; H, 4.39; N, 12.79.

Docking study

All ligands were drawn and optimized using Amber10 force field equation and Hamiltonian PM3, RHF and then saved as PDB file to use in docking simulation. Crystal structures of tubulin in complex with small molecule inhibitors vas retrieved from the RCSB protein data bank. All breaks and imperfections of crystal structure were corrected by comparing the sequence of amino acids using homology modeling. The missing parts of loop and terminal amino acids were added, the structure was protonated and partial charge was fixed, then the structure was energy minimized using amber10 force field equation. The optimized receptor and ligands were used for molecular docking studies using Autodock 4.2 software. Induce fit and Genetic algorithm was used to pose the proper conformation of compounds in the active site. Amber10 force field equation along with the calculation of hydrogen bonds and entropy changes were used to rate the best conformations. The results was analyzed using Discovery studio 4.5 and MOE software.

Biological Studies

Cell Culture

HT29, MCF-7, T47D, and NIH-3T3 (mouse embryonic fibroblast) cell lines were purchased from the Pasteur Institute (Tehran, Iran). The cells were cultured in RPMI-1640 medium (Sigma Aldrich, USA) supplemented with penicillin (100U/mL), streptomycin (100 µg/mL) and 10% heat-inactivated fetal bovine serum (Gibco, USA), at 37 °C in an incubator with 5% CO_2.

Cytotoxic Studies

The seeded cells (1000 cells per well density) was incubated in a 96 well plates for 24 h. Different concentration of the synthesized compounds at a range of 0.1-100 µM were added to the attached cultured cells and were incubated for 48 h. The plates were incubated for an extra 4 h after adding the Phosphate Buffered Saline solution (PBS) and MTT solution (5 mg/mL). The medium was removed and 100 µL of DMSO was added to each well for dissolving the formozan salt. In each plate, the absorbance was determined by an Anthous 2020 plate reader at 540 nm. The triplicated assay was performed and the IC_{50} values were determined by a nonlinear regression analysis.[22]

ACKNOWLEDGEMENTS

The authors declare no conflict of interest.

The current work was financially supported by Tehran University of Medical Sciences (GN: 9611302002).

REFERENCES

1. M. Kavallaris, *Nat. Rev. Cancer*, 2010, **10**, 194.
2. J. Zhou and P. Giannakakou, *Curr. Med. Chem. Anticancer Agents*, 2005, **5**, 65.
3. J. W. Hammond, D. Cai, and K. J. Verhey, *Curr. Opin. Cell Biol*., 2008, **20**, 71.
4. N. j. Cone, R. Miller, and N. Neuss, *J. Pharm. Sci.*, 1963, **52**, 688.
5. E. Nogales, S. G. Wolf, I. A. Khan, R. F. Luduena, and K. H. Downing, *Nature*, 1995, **375**, 424.
6. B. Gigant, C. Wang, R. B. Ravelli, F. Roussi, M. O. Steinmetz, P. A. Curmi, A. Sobel, and M. Knossow, *Nature*, 2005, **435**, 519.
7. R. B. Ravelli, B. Gigant, P. A. Curmi, I. Jourdain, S. Lachkar, A. Sobel, and M. Knossow, *Nature*, 2004, **428**, 198.
8. A. E. Prota, K. Bargsten, P. T. Northcote, M. Marsh, K. H. Altmann, J. H. Miller, J. F. Diaz, and M. O. Steinmetz, *Angew. Chem. Int. Ed.*, 2014, **53**, 1621.
9. A. E. Prota, K. Bargsten, J. F. Diaz, M. Marsh, C. Cuevas, M. Liniger, C. Neuhaus, J. M. Andreu, K. H. Altmann, and M. O. Steinmetz, *Proc. Natl. Acad. Sci. USA*, 2014, **111**, 13817.
10. Y. Lu, J. Chen, M. Xiao, W. Li, and D. D. Miller, *Pharm. Res*., 2012, **29**, 2943.
11. E. F. Hartung, *Ann. Rheum. Dis*., 1954, **13**, 190.
12. R. C. Weisenberg, G. G. Borisy, and E. W. Taylor, *Biochem*., 1968, **7**, 4466.
13. A. Dorleans, B. Gigant, R. B. Ravelli, P. Mailliet, V. Mikol, and M. Knossow, *Proc. Natl. Acad. Sci. USA*, 2009, **106**, 13775.
14. P. Barbier, A. Dorleans, F. Devred, L. Sanz, D. Allegro, C. Alfonso, M. Knossow, V. Peyrot, and J. M. Andreu, *J. Biol. Chem*., 2010, **285**, 31672.
15. A. E. Prota, F. Danel, F. Bachmann, K. Bargsten, R. M. Buey, J. Pohlmann, S. Reinelt, H. Lane, and M. O. Steinmetz, *J. Mol. Biol*., 2014, **426**, 1848.
16. D. Mengqi, L. Fang, Z. Hongyu, Z. Shumei, and Y. Bing, *Molecules*, 2016, **21**, 1375.
17. Y. Wang, H. Zhang, B. Gigant, Y. Yu, Y. Wu, X. Chen, Q. Lai, Z. Yang, Q. Chen, and J. Yang, *FEBS J*., 2016, **283**, 102.
18. N. Zhao, Z. L. Li, D. H. Li, Y. T. Sun, D. T. Shan, J. Bai, Y. H. Pei, Y. K. Jing, and H. M. Hua, *Phytochemistry*, 2015, **109**, 133.
19. M. Mahdavi, K. Pedrood, M. Safavi, M. Saeedi, M. Pordeli, S. K. Ardestani, S. Emami, M. Adib, A. Foroumadi, and A. Shafiee, *Eur. J. Med. Chem*., 2015, **95**, 492.
20. A. Faraji, R. Motahari, Z. Hasanvand, T. O. Bakhshaiesh, M. Toolabi, S. Moghimi, L. Firoozpour, M. A. Boshagh, R. Rahmani, S. H. M. E. Ketabforoosh, H. R. Bijanzadeh, R. Esmaeili, and A. Foroumadi, *Bioorg. Chem*., 2020, **108**, 104553.
21. A. Assadieskandar, M. Amini, S. N. Ostad, G. H. Riazi, T. Cheraghi-Shavi, B. Shafiei, and A. Shafiee,

Bioorg. Med. Chem., 2013, **21**, 2703.

22. M. Salehi, S. N. Ostad, G. H. Riazi, A. Assadieskandar, T. Cheraghi-Shavi, A. Shafiee, and M. Amini. *Med. Chem. Res*., 2014, **23**, 1465.
23. H. Z. Li, H. Y. He, Y. Y. Han, X. Gu, L. He, Q. R. Qi, Y. L. Zhao, and L. Yang, *Molecules*, 2010, **15**, 9473.
24. E. Saeedian Moghadam, F. Saravani, S. N. Ostad, S. Tavajohi, M. Pirali Hamedani, and M. Amini, *Heterocycl. Commun*., 2018, **24**, 211.
25. S. Saravani, E. Saeedian Moghadam, H. Salehabadi, S. N. Ostad, M. Pirali Hamedani, M. Amanlou, M. A. Faramarzi, and M. Amini, *Lett. Drug Des. Discov*., 2019, **16**, 1194.